Jessica Brandi[1]*
Ilaria Dando[2]*
Marta Palmieri[2]
Massimo Donadelli[2]
Daniela Cecconi[1]

[1]Proteomics and Mass Spectrometry Laboratory, Department of Biotechnology, University of Verona, Verona, Italy
[2]Biological Chemistry Section Department of Life and Reproduction Sciences, University of Verona, Verona, Italy

Received July 26, 2012
Revised February 7, 2013
Accepted February 8, 2013

Research Article

Comparative proteomic and phosphoproteomic profiling of pancreatic adenocarcinoma cells treated with CB1 or CB2 agonists

The pancreatic adenocarcinoma cell line Panc1 was treated with cannabinoid receptor ligands (arachidonylcyclopropylamide or GW405833) in order to elucidate the molecular mechanism of their anticancer effect. A proteomic approach was used to analyze the protein and phosphoprotein profiles. Western blot and functional data mining were also employed in order to validate results, classify proteins, and explore their potential relationships. We demonstrated that the two cannabinoids act through a widely common mechanism involving up- and down-regulation of proteins related to energetic metabolism and cell growth regulation. Overall, the results reported might contribute to the development of a therapy based on cannabinoids for pancreatic adenocarcinoma.

Keywords:
Cannabinoid / Pancreatic cancer / Proteomics DOI 10.1002/elps.201200402

Additional supporting information may be found in the online version of this article at the publisher's web-site

1 Introduction

Pancreatic adenocarcinoma is the fourth most common cause of cancer-related death in the world. The prognosis for patients affected by this type of cancer is poor, with the 5-year survival rate after diagnosis being less than 5% [1]. At present, the gold standard first-line therapy for patients with pancreatic adenocarcinoma is gemcitabine, a nucleoside analog of deoxycytidine, which inhibits DNA synthesis [2]. The unique mechanism of action and the favorable toxicity profile of gemcitabine have allowed explorations of new combined treatments based on this drug. Nevertheless, despite the progress made concerning the combination chemotherapy, mechanisms of resistance reduce the percentage of response: only 20% of patients have a 50% reduction of tumoral mass [3].

In recent years, cannabinoids and their derivatives have received considerable interest since they can affect the viability and invasiveness of different types of cancer cells [4]. Cannabinoids are bioactive lipids involved in a complex set of signaling pathways, mainly mediated by CB1 and CB2 receptors [5]. CB1 is the most abundant receptor in the central nervous system, and, besides its classical influence on mood and emotion, it has been demonstrated to play a role in the modulation of memory processing and in metabolism [6]. The related receptor, CB2, traditionally was thought to be expressed only in peripheral tissue, where it can help control inflammation and various immunological responses [7], but recent reports have suggested that it too can be found in the brain [8]. Both CB1 and CB2 are Gi/Go-protein-coupled receptors, the activation of which triggers inhibition of adenylyl cyclase and voltage-gated calcium channels, activation of potassium channels, mitogen-activated protein kinase, and phosphoinositide-3 kinase (PI3K)/Akt signaling pathways, induction of ceramide, and reactive oxygen species [5, 8].

Interestingly, CB1 and CB2 are overexpressed in pancreatic cancer tissue and cell lines and weakly or nonexpressed in normal pancreas [9]. This feature may constitute a good tool for both a potential use against pancreatic cancer and the elucidation of the signaling pathways mediated by CB1

Correspondence: Dr. Daniela Cecconi, Dipartimento di Biotecnologie, Laboratorio di Proteomica e Spettrometria di massa, Università degli Studi di Verona, Strada Le Grazie 15, 37134 Verona, Italy
E-mail: daniela.cecconi@univr.it
Fax: +39-045-8027929

Abbreviations: ACPA, arachidonylcyclopropylamide; **ANPEP**, alanine aminopeptidase; **ER**, endoplasmic reticulum; **GO**, gene ontology; **GW**, 1-(2,3-dichlorobenzoyl)-5-methoxy-2-methyl-3-[2-(4-morpholinyl)ethyl]-1H-indole; **PK**, pyruvate kinase; **WB**, Western blot

*These authors equally contributed to this work.

Colour Online: See the article online to view Figs. 2 and 4 in colour.

or CB2 activity. Donadelli et al. [10] have recently shown that association of gemcitabine with the synthetic cannabinoids arachidonylcyclopropamide (ACPA) or GW405833 (GW) synergistically inhibits pancreatic adenocarcinoma cell growth by increasing reactive oxygen species, endoplasmic reticulum (ER) stress and autophagic cell death. ACPA is a potent, stable, and selective agonist for CB1, 325 times more potent at CB1 compared to CB2, while GW is highly selective for CB2. The elucidation of the molecular mechanisms activated by CB1 or CB2 to influence pancreatic cancer cell proliferation has not been clarified and could be investigated by using the two selective agonists, ACPA and GW, and proteomic analyses.

The aim of this study was to shed light on the mechanism of action of ACPA and GW, and identify proteins and phosphoproteins that are modulated after treatment with the two cannabinoid receptor ligands in the Panc1 human pancreatic adenocarcinoma cell line.

2 Material and methods

2.1 Chemicals

ACPA was obtained from Cayman Chemicals (Inalco, Milan, Italy), and 1-(2,3-dichlorobenzoyl)-2-methyl-3-(2-(1-morpholine)ethyl)-5-methoxyindole (GW) from Sigma-Aldrich (Milan, Italy).

2.2 Cell culture

Panc1 human pancreatic adenocarcinoma cell line was grown in RPMI 1640 supplemented with 2 mM glutamine, 10% FBS and 50 μg/mL gentamicin sulfate (BioWhittaker, Italy) and incubated at 37°C with 5% CO_2.

2.3 Cell proliferation assay

Panc1 cells were plated in 96-well cell culture plates (5×10^3 cells/well), treated with ACPA and GW for 12 h at the indicated concentrations, and then stained with crystal violet (Sigma). The dye was solubilized in 1% SDS in PBS and measured photometrically (A_{595nm}) to determine cell growth. Four independent experiments were performed for each assay condition. The statistical analysis was performed with ANOVA (post hoc Bonferroni) using GraphPad Prism 5.

2.4 Protein sample preparation

For 2DE analysis, 1.2×10^6 cells were plated into five 10 cm dishes for each sample, starting from the same cell culture. After 24 h, cells were treated with 200 μM GW or ACPA for 12 h. This process was performed four independent times. Protein extraction was performed in a 2DE buffer containing 7 M urea (Sigma), 2 M thiourea (Sigma), 3% CHAPS (Sigma), 40 mM Tris (Sigma), and protease inhibitor cocktail (Complete, Mini; Roche, Basel, Switzerland). Cells were lysated by a sonicator tip through five applications of 30 s and intervals on ice, then pH 3–10 Ampholyte (Fluka, Buchs, SG, Switzerland) was added to remove the complexed nucleic acids by centrifugation (40 min at 14 000 × *g*). Protein fractions were then precipitated by acetone/methanol, pelleted by centrifugation at 14 000 × *g* for 40 min at 4°C, and resuspended in 2DE buffer. Samples were incubated with 5 mM tributyl phosphine and 20 mM acrylamide for 60 min at room temperature to reduce protein disulphide bonds and alkylate sulfhydryl groups. The reaction was blocked by 10 mM DTT and samples were stored at –80°C. Protein concentration was evaluated with Bradford assay (Bio-Rad).

2.5 Two-dimensional electrophoresis

Protein fractionation was performed as previously described [11] by using 17 cm IPG strips pH 3–10 (loaded with 900 μg of total protein) and 8–18%T SDS-PAGE. Detection of putative phosphoproteins was obtained by fixing the gels in 50% methanol and 10% acetic acid and, after washing, by an overnight staining with Pro-Q Diamond (Invitrogen, Molecular Probes). Gel images were recorded using a Typhoon 9600 scanner (GE Healthcare, San Francisco, CA). Total proteins were then revealed by an overnight incubation with Sypro Ruby stain (Sigma) and then by destaining in 10% methanol and 7% acetic acid for 1 h. Total protein spots were detected by Versa-Doc Model 1000 (Bio-Rad).

The protein pattern differential analysis of 15 stained gels (five technical replicates × three samples, i.e. control, ACPA and GW treated cells) of the two dataset (phosphoproteome and total proteome) were performed by PDQuest software v7.3 (Bio-Rad) as previously described [11]. Differentially expressed proteins and phosphoproteins were considered significant at p-value <0.05 and the change in OD of spots had to be >2-fold.

2.6 Protein identification by nano-HPLC-Chip IT MS/MS

Protein identification was performed after in-gel trypsin digestion as previously described [12]. Briefly, peptides from each sample were separated by RP nano-HPLC-Chip technology (Agilent Technologies, Palo Alto, CA, USA) online-coupled with a 3D IT mass spectrometer (model Esquire 6000, Bruker Daltonics, Bremen, Germany). Database searches were conducted using the MS/MS ion search of Mascot against human entries of the nonredundant NCBI database, with propionamide formation of cysteines as fixed modification and oxidized methionine, acetylated protein *N* terminus, and phosphorylation of serine, threonine, and tyrosine as variable modifications. Trypsin was specified as the proteolytic enzyme and one missed cleavage was allowed. The

mass tolerance of the precursor and fragment ions was set to ±0.9 Da. Positive identification was determined if Mascot score was significant ($p < 0.05$) and at least two peptides matched the same protein.

2.7 Western blot analysis

Protein validation by Western blot (WB) analysis was performed as previously described [13]. Briefly, proteins were resuspended with Laemmli's sample buffer, separated on 12%T SDS-PAGE and then transferred to a PVDF membrane (60 V for 2 h at 4°C). After blocking of nonspecific sites by TBST-milk solution, membranes were treated with primary and secondary antibodies at the appropriate dilutions (see the Supporting Information Table 1) in 1% nonfat dried milk, 0.05% Tween-20 TBS. The immunocomplexes were detected by ECL (Amersham Biosciences) by a ChemiDoc instrument (Bio-Rad).

2.8 Functional data mining

Functional annotation was performed according to gene ontology (GO) using the FatiGO tool from Babelomics 4.2 (http://babelomics.bioinfo.cipf.es/fatigo.html). The enrichment analysis for cellular component, biological process, and molecular function was done by comparing the GO terms of identified proteins against the rest of the genome. The Fisher's exact test detected the significant overrepresentation of GO terms in the submitted dataset [14]. We conducted also an enrichment analysis for KEGG pathways [15].

In silico characterization of phosphorylation sites by NetPhos 2.0, PhosphoBase 9.0, and Scansite 3.0 was instead performed as previously described [16]. Protein interactions were assessed using the STRING database (http://string-db.org) in order to show connection among all the modulated proteins and phosphoproteins. We retrieved interactions that were of at least high confidence (score 0.7) based exclusively on experimental and database knowledge while excluding all other prediction methods implemented in STRING (such as textmining and coexpression). Additional white nodes to 10 (as to reduce noise) and network depth were kept to the minimum value (1), in order to exclude as many false-positive interactions as possible.

3 Results

3.1 Inhibition of proliferation of Panc1 cells by ACPA or GW

The antiproliferative effect of the synthetic cannabinoids ACPA or GW was examined after treatment for 12 h with increasing amounts of the compounds. Figure 1 shows that both cannabinoids were able to inhibit cell growth, being

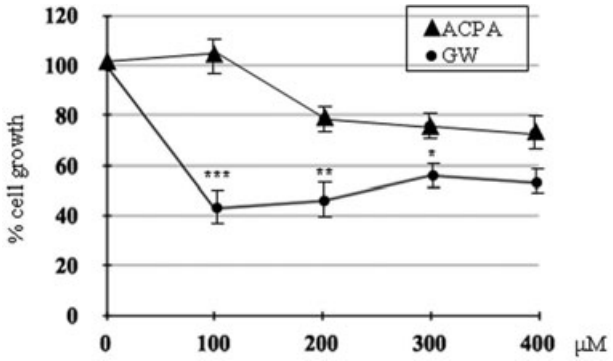

Figure 1. Growth inhibition of Panc1 cells with increasing concentrations of ACPA or GW at 12 h. ***$p < 0.001$, **$p < 0.01$, and *$p < 0.05$.

GW significantly more active than ACPA. However, the cell growth curve reached a plateau at 100 μM with GW and at 200 μM with ACPA. For this reason, proteomic study was performed using a concentration of 200 μM for both cannabinoids.

3.2 Proteome and phosphoproteome modulation of Panc1 cells treated with ACPA or GW

To expand the knowledge of the molecular mechanisms involved in ACPA or GW induced cell death, we analyzed the total proteome and the phosphoproteome of Panc1 cells (representative maps are shown in Supporting Information Fig. 1). Three analyses were performed: (i) ACPA/control; (ii) GW/control; and (iii) GW/ACPA. After normalization of the gels, 62 spots displayed significantly altered intensities ($p < 0.05$, *t*-test) and were analyzed by MS/MS. The following numbers of spots were identified: ACPA/control, 24 phosphoproteins and 21 proteins; GW/control, 27 phosphoproteins and 14 proteins; GW/ACPA, 12 phosphoproteins and 14 proteins. The overlap of unique identified proteins and phosphoproteins between the three comparisons is shown in Fig. 2, while master maps indicating the identified proteins and phosphoproteins are reported in Supporting Information Fig. 2. The MS proteomics data have been deposited to the ProteomeXchange Consortium (http://proteomecentral.proteomexchange.org) via the PRIDE partner repository [17] with the dataset identifier PXD000119 and DOI 10.6019/PXD000119 and are also listed in the Supporting Information Table 2. It must be taken into account that all the phosphoproteins for which it was not possible to determine at least a phosphorylation site by MS/MS analysis should be considered as putatively phosphorylated.

In order to confirm the proteomic data, the modulation of pyruvate kinase (PKM2), phosphopyruvate kinase (p-PKM2, Tyr-105), keratin 18 (KRT18), phosphokeratins 18 (Ser-33 and Ser-52, p-KRT18) was analyzed by WB. The 2DE spots corresponding to the immunodetected proteins are shown in Fig. 3A.

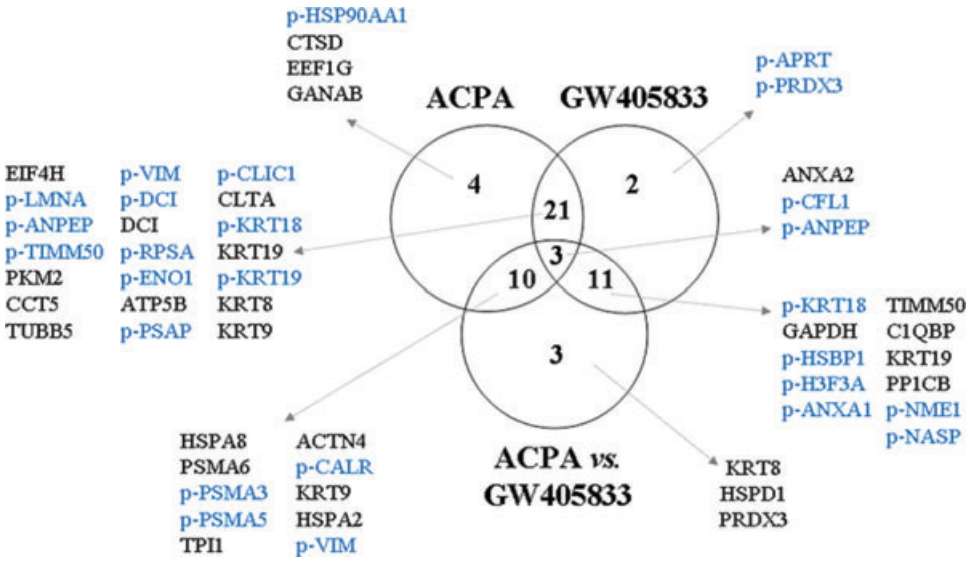

Figure 2. The overlap of proteins identified across all three comparisons: ACPA/control, GW/control, and GW/ACPA, respectively.

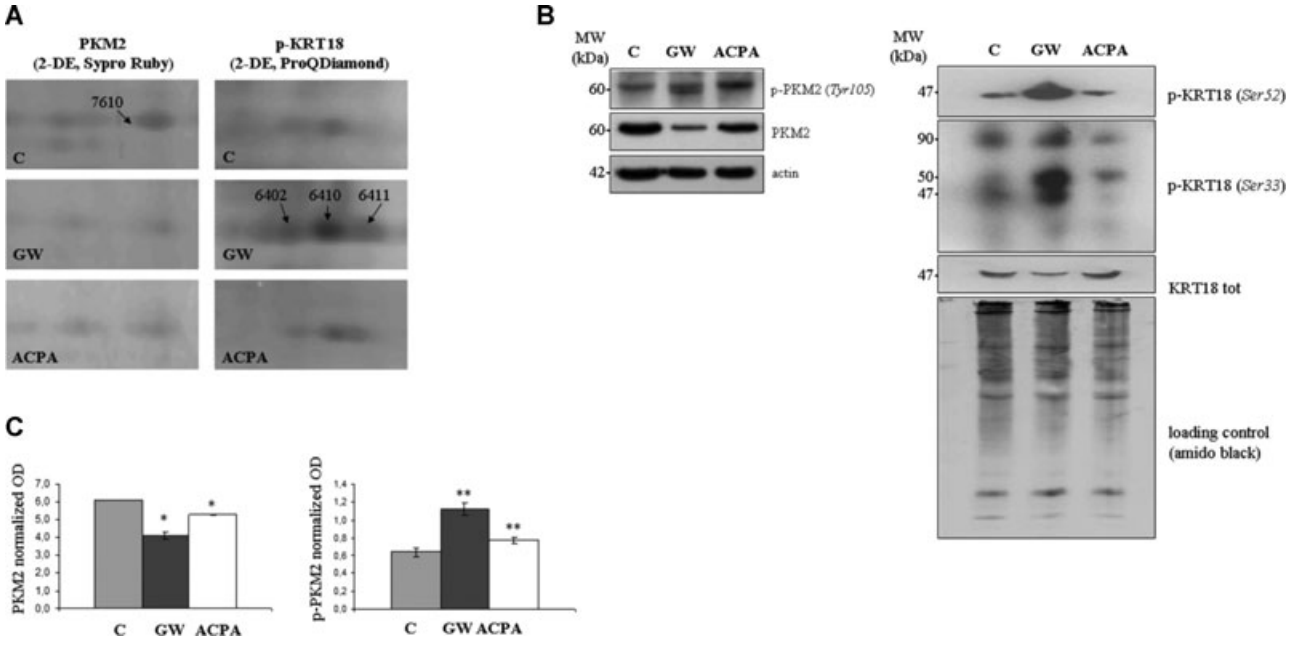

Figure 3. (A) Zooms of 2DE spots corresponding to the immunodetected proteins. (B) Western blot obtained using anti-p-PKM2 (Tyr 105), anti-PKM2, anti-p-KRT18 (Ser52), anti-p-KRT18 (Ser33), and anti-KRT18 antibodies to probe protein extracts from Panc1 cells after 12 h of treatment with GW or ACPA. (C) Band densitometry (statistics: two-tailed *t*-test) showing amount of the PKM2 (normalized to actin) and p-PKM2 (normalized to actin and to PKM2). ***$p < 0.001$, **$p < 0.01$, and *$p < 0.05$.

Figure 3B reports that p-PKM2 (Tyr105) and total PKM2 are respectively up- and downregulated in GW as well as in ACPA treated cells, while p-KRT18 (Ser 52 and Ser33) and KRT18 are respectively up- and downregulated in particular in GW-treated cells (and only slightly after ACPA treatment). In particular, densitometric analysis of immunodetected PKM2 (normalized to actin) revealed that it is downregulated 1.16 ± 0.03-fold by ACPA and 1.50 ± 0.08-fold by GW; while p-PKM2 (normalized to actin and then to total PKM2) is upregulated 1.21 ± 0.02-fold by ACPA and 1.76 ± 0.03-fold by GW (Fig. 3C). Surprisingly, the downregulation of PKM2 was less evident in ACPA probably due to the overlap of more isoforms (nonsignificant in 2DE) that may have an opposite modulation.

3.3 Bioinformatics and protein–protein interaction analyses

By bioinformatics, we found that the cellular components mostly overrepresented in cannabinoid-treated cells were the soluble fraction, membrane-bounded vesicles, vesicles, and

Table 1. Significantly enriched ontologies in Panc1-treated cells

Term	Pivotal proteins	#1 vs. # rest of the genome (%)	Adjusted *p* value ($p < 0.005$)
Biological process			
Interspecies interaction between organisms (GO:0044419)	KRT18, KRT19, KRT8, EIF4H, HSPD1, HSPA8, ANPEP, C1QBP, VIM	20.45 vs. 1.42	0.00002643
Response to unfolded protein (GO:0006986)	CLIC1, HSPD1, HSPB1, HSP90AB1, HSPA2, HSPA8	13.64 vs. 0.49	0.0001108
Response to biotic stimulus (GO:0009607)	CTSD, CLIC1, KRT8, HSPD1, HSPB1, HSP90AB1, HSPA2, HSPA8, PRDX3	20.45 vs. 2	0.0001157
Response to organic substance (GO:0010033)	CLIC1, CFL1, KRT19, HSPD1, HSPB1, HSP90AB1, HSPA2, HSPA8, NME1, PKM2, PRDX3	25 vs. 3.33	0.0001157
Response to protein stimulus (GO:0051789)	CLIC1, HSPD1, HSPB1, HSP90AB1, HSPA2, HSPA8	13.64 vs. 0.65	0.0002126
Membrane organization (GO:0016044)	ACTN4, ATP5B, CALR, CLTA, LMNA, TIMM50, NME1	15.91 vs. 1.68	0.002835
Glycolysis (GO:0006096)	ENO1, GAPDH, PKM2, TPI1	9.09 vs. 0.27	0.002835
Molecular function			
Unfolded protein binding (GO:0051082)	CALR, HSPD1, HSP90AB1, HSPA2, HSPA8, CCT5	13.64 vs. 0.55	0.0001897
Cellular component			
Soluble fraction (GO:0005625)	ANXA2, CTSD, CLTA, GANAB, HSPD1, HSP90AB1, HSPA8, ANPEP	15.91 vs. 1.4	0.0001131
Membrane-bounded vesicle (GO:0031988)	ANXA2, CTSD, CLTA, GANAB, HSPD1, HSP90AB1, HSPA8, ANPEP	18.18 vs. 2.25	0.0001233
Vesicle (GO:0031982)	ANXA2, CTSD, CLTA, GANAB, HSPD1, HSP90AB1, HSPA8, ANPEP	18.18 vs. 2.83	0.0004169
Cell surface (GO:0009986)	ANXA2, CTSD, CLTA, GANAB, HSPD1, HSP90AB1, HSPA8, ANPEP	13.64 vs. 1.45	0.0004355

cell surface. In addition, the GO enrichment analysis suggests that the identified proteins are involved in interactions between organisms, in response to stimuli (such as protein, biotic, and organic substances), in membrane organization, and in glycolysis. As concerning statistically enriched GO term in the category "molecular function," we found significant the term unfolded protein binding (Table 1).

Furthermore, an enrichment analysis was performed to find which cellular KEGG pathways could be affected by ACPA and/or GW exposure in Panc1 cells. The results obtained revealed a total of three altered KEGG pathways: glycolysis/gluconeogenesis (hsa00010, adjusted *p*-value = 9.189×10^{-4}), antigen processing and presentation (hsa04612, adjusted *p*-value = 0.014), and proteasome (hsa03050, adjusted *p*-value = 0.0014).

By STRING analysis, we identified a core network of modulated proteins and putative phosphoproteins involved in the energetic metabolism (PKM2, ENO1, NME1, ATP5B, GAPDH, TPI1), and one composed of structural proteins (i.e. KRT1, KRT8, KRT18, KRT19, VIM, and LMNA). Another central group of the data shows interaction among clathrin light chain A (CLTA), chaperones (HSPA8, HSP90AB1, HSPD1), and proteasome subunits (PSMA3, PSMA5, PSMA6), suggesting modulation of protein turnover. Figure 4 shows the stronger associations between these proteins by thicker lines.

For all the identified putative phosphoproteins, a number of phosphorylation sites were predicted by Netphos 2.0. The Phosphobase 9.0 search provided the determination of the exact position of the known phosphorylation sites based on the available literature. While by Scansite 3.0 analysis, potential-binding sites for members of the ERK 1/2 kinase (29%) and casein kinase (21%) family were most commonly predicted in identified phosphoproteins (see Supporting Information Table 2).

4 Discussion

4.1 ACPA and GW alter the amount of proteins involved in the energetic metabolism and cell growth regulation

The identification of the energetic metabolism as a central node in the STRING analysis, as well as a statistically significant prominence of glycolysis in the GO terms enrichment analysis suggest this may be an important target for the mechanism of action of ACPA and GW. Pyruvate kinase (PK) catalyzes the final step of glycolysis, generating ATP and pyruvate. Different isozymes of PK are expressed in relation to the metabolic characteristics of the various cells and tissues, such as L-PK (liver and kidneys), R-PK (erythrocytes), PKM1 (muscles and brain), and PKM2 (lung, fat tissue, retina, and pancreatic islets, as well as cells with a high rate of nucleic acid synthesis, such as normal proliferating, embryonic, and tumour cells). PKM2 fluctuates between two major states: an active tetrameric form and a less active dimer. In tumor cells, PKM2 establishes whether glucose is converted to lactate for regeneration of energy (active tetrameric form, Warburg effect) or used for the synthesis of cell-building blocks (nearly inactive dimeric form) [18]. Multiple mechanisms lead to

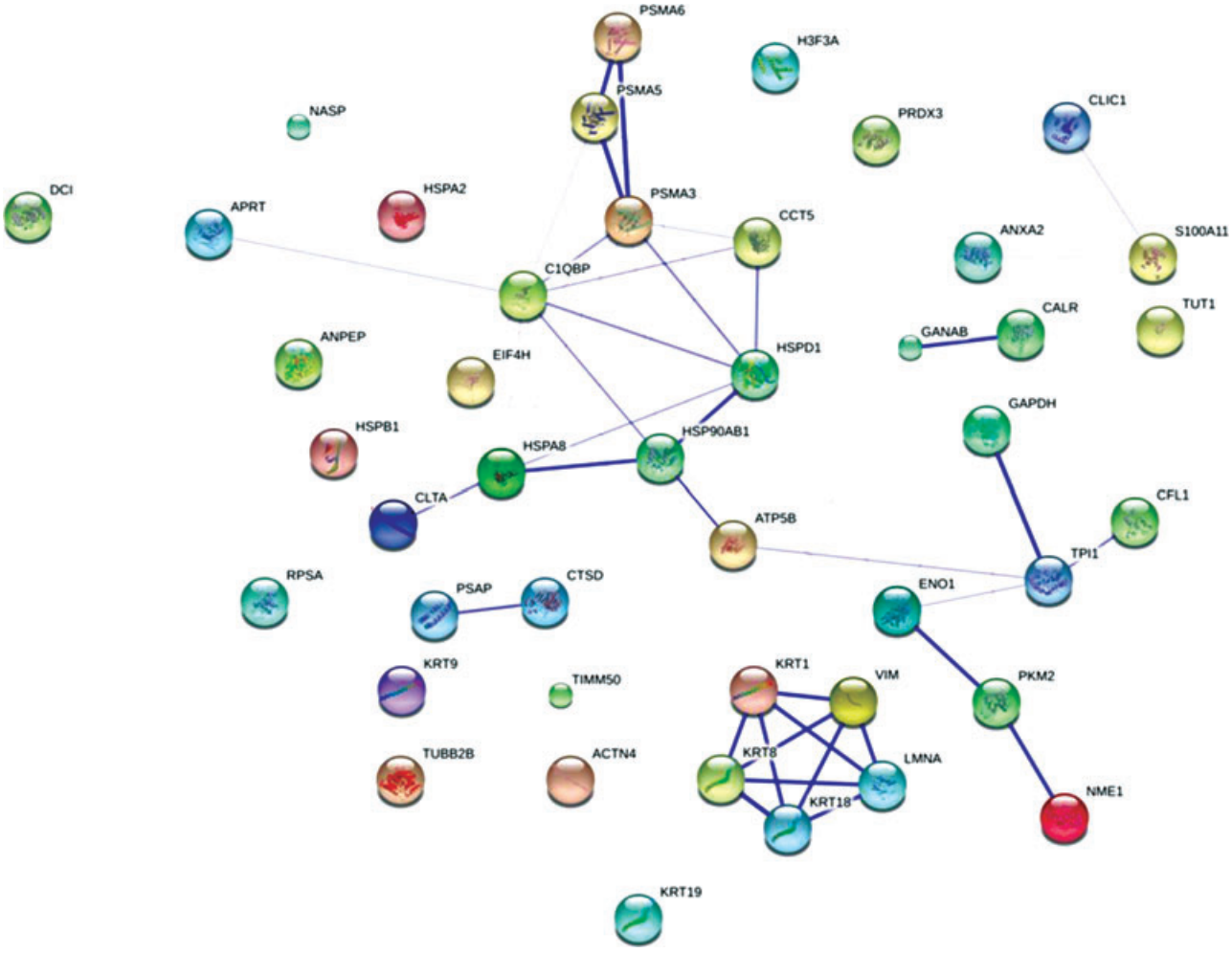

Figure 4. STRING 9.0 protein interaction network for the identified proteins, stronger associations are represented by thicker lines.

inhibition of the tetrameric PKM2 active form: phosphorylation at Tyr105 [19], binding to tyrosine phosphorylated polypeptides, oxidation of Cys358, and acetylation on Lys305. PKM2 has also nonmetabolic functions in the control of cell-cycle progression (by inducing the expression of cyclin D1) [20] and in transcription of MEK5 [21] an upstream activator of ERK5 (an homolog of ERK1/2) mediating the effects of a number of oncogenes. Accordingly, we confirm by Scansite analysis that cannabinoid action imply ERK 1/2 regulation. The 2DE results indicated that the amount of one form of PKM2 protein is downregulated (<20-fold, SSP7610) by both ACPA and GW treatments, while WB results indicated a less marked reduction of total PKM2 (Fig. 3B). This discrepancy could be attributed to the lower resolving power of 1D-WB (as compared to 2DE), which is not able to separate all the different forms of a protein (i.e. subjected to different PTMs). By immunoblot analysis (Fig. 3B), we also revealed that p-PKM2 (Tyr 105) is induced by both treatments, particularly by GW.

The data obtained suggest that ACPA and GW, by downregulating the amount of one particular form of PKM2 and switching the enzyme into its inactive dimeric form (Tyr105 phosphorylated), could represent effective inhibitors of aerobic glycolysis (Warburg effect). By considering the different abilities especially in inducing p-PKM2, it is possible to argue that GW has a more pronounced effect in inhibiting the aerobic glycolysis. Interestingly, it has been reported that knockdown of PKM2 by RNA interference induces apoptosis and tumor regression [22] and that PKM2 inhibition with peptide aptamers inhibits cell proliferation [23].

The inhibition of glycolysis depletes ATP in cancer cells, especially cells with mitochondrial respiration defects, leads to dephosphorylation of the glycolysis-apoptosis integrating molecule BAD, relocalization of BAX to mitochondria, and massive cell death [24]. Interactome analysis (Fig. 4) suggests that PKM2 is strongly linked to alpha enolase (ENO1), another enzyme involved in glycolysis. We found that the phosphorylated isoform of ENO1 (SSP7504) is downregulated by both ACPA (–5.6-fold) and GW (–4.2-fold) treatments. ENO1 phosphorylation is strongly associated with pancreatic cancer, and induces specific autoantibodies in patients that may have diagnostic value [25].

Adhesive interactions of tumor cells with the surrounding microenvironment represent a crucial parameter within growth, migration, and metastasis of cancer cells. Interestingly, some although still rare correlations between activation of the cannabinoid receptors CB1 [26–28] and CB2 [29, 30] and suppression of adhesion molecules have been reported. Our findings imply a downregulation of phosphorylated isoform of 67 kDa receptor of laminin (RSPA) (<20-fold, SSP3408) after treatment of pancreatic cancer cells with ACPA and GW. RPSA represents a prognostic biomarker for a variety of human cancers and is involved in cell adhesion to the basement membrane. The interaction of cancer cells with laminin is in fact a key event in tumor invasion and metastasis able to induce tumor cell proliferation [31].

Treatment of Panc-1 cells with cannabinoids strongly downregulates phosphorylated alanine aminopeptidase (ANPEP) (<20-fold, SSP3901). ANPEP is a zinc-dependent metallo-exopeptidase, overexpressed on the surface of different tumor cells [32], which degrades the extracellular matrix, inducing tumor invasion, angiogenesis, and metastasis. It is a transcriptional target of Ras signaling pathways in endothelial morphogenesis. Recently, several ANPEP inhibitors have been developed and some of them have been found to have effectiveness as anti-cancer agents [33]. Interestingly, ANPEP has also been proposed as a new prognostic marker for patients with pancreatic carcinoma [34].

Our data show that cannabinoids induce different isoforms of phospho-keratins 18 (KRT18) (SSP6411, SSP6402, SSP6410). KRT18 is an intermediate filament protein involved in invasion, apoptosis, mitosis, cell-cycle progression, and signaling. Phosphorylation of KRT18 at Ser52 is important for filament reorganization during mitotic arrest [35]. In particular, during apoptosis, intermediate filaments reorganize into granular structures enriched for KRT18 phosphorylated on serine 52. Phosphorylation of KRT18 at Ser33 is instead essential for its association with 14–3–3 proteins but seems to be not important for apoptotic cell death [36]. Here, we demonstrated that cannabinoid agonists, and in particular GW, strongly induces KRT18 phosphorylation at Ser52 and Ser33, while total KRT18 is downregulated (Fig. 3B). These findings suggest that activation of CB2 receptor, by increasing phosphorylation of KRT18 leads to collapse of the keratin cytoskeleton and cell death [37].

The mechanism of action of ACPA and GW also imply the upregulation of the phosphorylated isoform of prosaposin (PSAP) (>20-fold, SSP2004). Notably, expression of PSAP is reduced in metastatic cancer cell lines [38], and enhanced tumor cell secretion of PSAP inhibits the metastatic process via stimulation of stromal p53 and thrombospondin-1 (an adhesive glycoprotein that mediates cell-to-cell and cell-to-matrix interactions) [39]. In addition, PSAP activates the phosphorylation of ERK 1/2 isoforms [40], which are involved in the cannabinoid mechanism of action [41], and were found by Scansite analysis as the main kinases involved in the phosphorylation of identified proteins. PSAP is proteolytically cleaved into saposins A, B, C, and D, which function as cofactors for sphingolipid hydrolases. The p-PSAP upregulation we detected could support the antiproliferative effect of ACPA and GW treatments on Panc1 cells and confirm an involvement of these cannabinoids in tumor metastasis reduction.

As concerning an involvement of autophagic cell death in the mechanism of action of ACPA and GW a first indication is given by the GO enrichment analysis, which detected overrepresented proteins belonging to membrane-bounded vesicle and vesicles (Table 1). The importance of autophagy in cannabinoid action is confirmed by modulation of clathrin, in particular of clathrin light chain A (CLTA, SSP1203) that is upregulated by both ACPA (+2.7-fold) and GW (+2-fold) treatments. CLTA is directly involved in autophagic process: the endocytic plasma membrane-derived clathrin coated vesicles form phagophore precursor structures, which are expanded to become autophagosomes, which fuse with endosomes and lysosomes to degrade their contents [42].

4.2 ACPA regulates folding and proteolytic turnover of proteins, as well as autophagy-mediated cell death

The activation of CB1 receptor by ACPA specifically upregulates cathepsin D, elongation factor 1-gamma, glucosidase II, phospho-hsp90 kDa, hsp70 kDa protein 2 and protein 8, phosphorylated proteasome subunit alpha type-3, and triosephosphate isomerase 1, chain A. Moreover, induction of CB1 signaling by ACPA leads to downregulation of alpha actinin 4, phospho-calreticulin, one isoform of hsp70 protein 8, proteasome subunit alpha type-6 and phospho-alpha type-5, as well as one protein form of vimentin.

The proteasome pathway plays an important role in cellular homeostasis and in a variety of cellular pathways, including cell growth and proliferation, apoptosis, and DNA repair. Accordingly, proteasome inhibitors are being studied in the treatment of different types of cancer including pancreatic cancer [43]. We have shown that ACPA downregulates two proteasome subunits, PSMA6 (–4.5-fold, SSP 5210) and p-PSMA5 (–5.9-fold, SSP 3305) suggesting that ACPA antitumor activity also depends on deregulation of proteasome proteolytic pathway. However, this mechanism of action may have only a marginal role, as ACPA treatment also leads to a strong induction of p-PSMA3 (>20-fold, SSP5314).

Lysosomal enzymes, such as lysosomal aspartyl proteases named cathepsins, are also implicated in protein degradation and turnover. Recently, it has been also demonstrated that high expression of cathepsin D (CTSD) activates autophagy with increasing of acidic autophagic vacuoles and LC3-II formation [44]. Our results revealed that activation of CB1 receptor by ACPA is related to upregulation of CTSD (+2-fold, SSP4211) further indicating the importance of the autophagic process in cell death induced by CB1-selective agonist [10].

The "calnexin/calreticulin cycle" is a quality control system responsible for promoting the folding of newly synthesized glycoproteins entering the ER [45]. Nascent and newly synthesized glycoproteins enter the calnexin/calreticulin (CALR) cycle when two of three glucoses in the core

N-linked glycans have been trimmed by ER glucosidase II (GANAB). The functional association between CALR and GANAB was confirmed also by interactome analysis (Fig. 4). Taken together, our results indicate a deregulation of "calnexin/calreticulin cycle": we found two phosphorylated isoforms of CALR, having a M_r almost tripled (about 70 kDa instead of 24 kDa), which are downregulated (both –2.3-fold, SSP2603, and SSP2604), and one overexpressed isoform of GANAB (+2.7-fold, SSP4807). In addition, CALR promotes the expression of adhesion molecules (ICAM-1 and VCAM-1) on tumor cells [46], and its knockdown suppresses cancer cell proliferation, migration, and metastatic capacities [47]. The CALR downregulation we report seems to be in line also with the anti-invasive effect we have already described above as common mechanism between ACPA and GW. It remains to be explained the meaning of CALR phosphorylation and of its higher molecular mass.

As concerning modulated chaperones (hsp70 and hsp90), they have a role in chaperone-mediated autophagy (CMA) that is a selective form of autophagy where proteins are translocated directly from the cytosol across the lysosomal membrane for degradation inside lysosomes. CMA substrates are cytosolic proteins bearing a pentapeptide motif that, when recognized by the cytosolic chaperone hsp70 kDa protein 8 (HSPA8, also named Hsc70), targets them to the surface of the lysosomes [48]. HSPA8 is also involved in microautophagy: it delivers autophagic cargo to late endosomes for complete or partial degradation [49]. Also hsp70 kDa protein 2 (HSPA2, named hsp 70–2) is involved in CMA [50]. In addition, it has been reported that a complex form by hsp90 (and co-chaperone Cdc37) regulates the Ulk1- and Atg13-mediated mitophagy [51] (i.e. autophagy selective for degradation of mitochondria). Our results revealed that ACPA upregulates the level of amount of HSPA8 (>2.4-fold, SSP2708), HSPA2 (>2.1-fold, SSP1709), and p-HSP90 (+2.7-fold, SSP3810) confirming the key role of the autophagic process in cell death induced by CB1-selective agonist. On the contrary, one isoform of HSPA8 is instead downregulated (<2.3-fold, SSP4701), so it remains to be characterized from a functional point of view.

4.3 GW regulates bioenergetic signature, DNA, and histone metabolism, as well as autophagy-mediated cell death

The activation of CB2 receptor by GW specifically upregulates mitochondrial matrix protein p32, one form of cytokeratin 19, phosphorylated nuclear autoantigenic sperm protein. In addition, it downregulates phophorylated adenine phosphoribosyltransferase, glyceraldehyde-3-phosphate dehydrogenase, protein phosphatase 1 catalytic subunit beta isoform, phospho-hsp27 kDa, phospho-annexin 1, phosphorylated histone H3, nucleoside diphosphate kinase A, and phosphorylated thioredoxin-dependent peroxide reductase.

Cancer aggressiveness can be estimated by its "bioenergetic signature" (i.e. the protein ratio β-F1-ATPase/GAPDH) [52] that provides an estimate of glucose metabolism in tumors and serves as a prognostic indicator for cancer patients. Along with the limitation of mitochondrial oxidative phosphorylation in different type of carcinomas, it has been observed an upregulation of the glycolytic GAPDH that was confirmed in pancreatic cancerous tissues [53]. Accordingly, we have shown that the antitumoral effect of GW is associated with downregulation of GAPDH (<2.5-fold, SSP 4303) implying a targeting of energetic metabolism.

Proper genome packaging requires coordination of both DNA and histone metabolism. In this respect, histone chaperone nuclear autoantigenic sperm protein (NASP) stabilizes a reservoir of soluble histones H3-H4 (required for the dynamic chromatin reorganization) by protecting them from degradation via CMA [54]. Here, we found that GW upregulates phospho-NASP (+3-fold, SSP2811) and downregulates phospho-histone H3 (H3F3A) (–2.8-fold, SSP 6105). We found that the GW also downregulates phosphorylated adenine phosphoribosyltransferase (APRT) (–3.1-fold, SSP 6202) and phosphorylated nucleoside diphosphate kinase (NME1) (–2.5-fold, SSP 7202). APRT is an enzyme involved in the purine nucleotide salvage pathway; it functions as a catalyst in the reaction between adenine and phosphoribosyl pyrophosphate to form AMP. NME1 is instead involved in the synthesis of nucleoside triphosphates other than ATP. Taken together our data suggest that mechanism of action of GW may involve regulation of nucleotide and histone metabolism.

Finally, GW upregulates (>2.4-fold, SSP 1202) the amount of mitochondrial matrix p32 protein (C1QBP). This protein not only supports oxidative phosphorylation but also promotes autophagic cell death [55]. C1QBP stabilizes the autophagic inducer smARF [56], which translocates to the mitochondria and dissipates the mitochondrial membrane potential inducing autophagic cell death [57]. In particular, C1QBP binds the ARF C terminus and is required for ARF to localize to mitochondria [58]. This finding may suggest that GW could exert a stronger induction of the autophagic cell death, as compared to ACPA, by upregulating C1QBP.

This work was supported by Associazione Italiana Ricerca Cancro (AIRC), Milan, Italy; Fondazione CariPaRo, Padova, Italy; Progetti di Ricerca di Interesse Nazionale (PRIN, MIUR), Rome, Italy.

The authors have declared no conlfict of interest.

5 References

[1] Vincent, A., Herman, J., Schulick, R., Hruban, R. H., Goggins, M., *Lancet* 2011, *378*, 607–620.

[2] Plunkett, W., Huang, P., Xu, Y. Z., Heinemann, V., Grunewald, R., Gandhi, V., *Semin. Oncol.* 1995, *22*, 3–10.

[3] Shi, X., Liu, S., Kleeff, J., Friess, H., Buchler, M. W., *Oncology* 2002, *62*, 354–362.

[4] Calvaruso, G., Pellerito, O., Notaro, A., Giuliano, M., *Int. J. Oncol.* 2012, *41*, 407–413.

[5] Pertwee, R. G., Howlett, A. C., Abood, M. E., Alexander, S. P., Di Marzo, V., Elphick, M. R., Greasley, P. J., Hansen, H. S., Kunos, G., Mackie K., Mechoulam R., Ross, R. A., *Pharmacol. Rev.* 2010, *62*, 588–631.

[6] Zanettini, C., Panlilio, L. V., Alicki, M., Goldberg, S. R., Haller, J., Yasar, S., *Front Behav. Neurosci.* 2011, *5*, 57.

[7] Klein, T. W., Newton, C., Larsen, K., Lu, L., Perkins, I., Nong, L., Friedman, H., *J. Leukoc. Biol.* 2003, *74*, 486–496.

[8] Svizenska, I., Dubovy, P., Sulcova, A., *Pharmacol. Biochem. Behav.* 2008, *90*, 501–511.

[9] Carracedo, A., Gironella, M., Lorente, M., Garcia, S., Guzmán, M., Velasco, G,. Iovanna, J. L., *Cancer Res.* 2006, *66*, 6748–6755.

[10] Donadelli, M., Dando, I., Zaniboni, T., Costanzo, C., Dalla Pozza, E., Scupoli, M. T., Scarpa, A., Zappavigna, S., Marra, M., Abbruzzese, A., Bifulco, M., Caraglia, M., Palmieri, M., *Cell Death Dis.* 2011, *2*, e152.

[11] Cecconi, D., Scarpa, A., Donadelli, M., Palmieri, M., Hamdan, M., Astner, H., Righetti, P. G., *Electrophoresis* 2003, *24*, 1871–1878.

[12] Millioni, R., Polati, R., Menini, M., Puricelli, L., Miuzzo, M., Tessari, P., Novelli, E., Righetti, P. G., Cecconi, D., *PLoS One* 2012, *7*, e30911.

[13] Cecconi, D., Lonardoni, F., Favretto, D., Cosmi, E., Tucci, M., Visentin, S., Cecchetto, G., Fais, P., Viel, G., Ferrara, S. D., *Electrophoresis* 2011, *32*, 3630–3637.

[14] Al-Shahrour, F., Diaz-Uriarte, R., Dopazo, J., *Bioinformatics* 2004, *20*, 578–580.

[15] Kanehisa, M., Araki, M., Goto, S., Hattori, M., Hirakawa, M., Itoh, M., Katayama, T., Kawashima, S., Okuda S., Tokimatsu, T., Yamanishi, Y., *Nucleic Acids Res.* 2008, *36*, D480–D484.

[16] Cecconi, D., Zamo, A., Bianchi, E., Parisi, A., Barbi, S., Milli, A., Rinalducci, S., Rosenwald, A., Hartmann, E., Zolla, L., Chilosi, M., *Proteomics* 2008, *8*, 4495–4506.

[17] Vizcaino, J. A., Cote, R., Reisinger, F., Barsnes, H., Foster, J. M., Rameseder, J., Hermjakob, H., Martens, L., *Nucleic Acids Res.* 2010, *38*, D736–D742.

[18] Chaneton, B., Gottlieb, E., *Trends Biochem. Sci.* 2012, *37*, 309–316.

[19] Hitosugi, T., Kang, S., Vander Heiden, M. G., Chung, T. W., Elf, S., Lythgoe, K., Dong, S., Lonial, S., Wang, X., Chen, G. Z., Xie, J., Gu, T. L., Polakiewicz, R. D., Roesel, J. L., Boggon, T. J., Khuri, F. R., Gilliland, D. G., Cantley, L. C., Kaufman, J., Chen, J., *Sci. Signal.* 2009, *2*, ra73.

[20] Canal, F., Perret, C., *Future Oncol.* 2012, *8*, 395–398.

[21] Gao, X., Wang, H., Yang, J. J., Liu, X., Liu, Z. R., *Mol. Cell.* 2012, *45*, 598–609.

[22] Goldberg, M. S., Sharp, P. A., *J. Exp. Med.* 2012, *209*, 217–224.

[23] Spoden, G. A., Mazurek, S., Morandell, D., Bacher, N., Ausserlechner, M. J, Dürr, P. D., Eigenbrodt E., Zwerschke, W., *Int. J. Cancer* 2008, *123*, 312–321.

[24] Xu, R. H., Pelicano, H., Zhou, Y., Carew, J. S., Feng, L., Bhalla, K. N., Keating, M. J., Huang, P., *Cancer Res.* 2005, *65*, 613–621.

[25] Tomaino, B., Cappello, P., Capello, M., Fredolini, C., Sperduti, I., Migliorini, P., Salacone, P., Novarino, A., Giacobino, A., Ciuffreda, L., Alessio, M., Nistico, P., Scarpa, A., Pederzoli, P., Zhou, W., Petricoin, E. F., Liotta, L. A., Giovarelli, M., Milella, M., Novelli F., *J. Proteome Res.* 2011, *10*, 105–112.

[26] Rossi, B., Zenaro, E., Angiari, S., Ottoboni, L., Bach, S., Piccio, L., Pietronigro, E. C., Scarpini, E., Fusco, M., Leon, A., Constantin, G., *J. Neuroimmunol.* 2011, *233*, 97–105.

[27] Grimaldi, C., Pisanti, S., Laezza, C., Malfitano, A. M., Santoro, A., Vitale, M., Caruso, M. G., Notarnicola, M., Iacuzzo, I., Portella, G., Di Marzo, V., Bifulco, M., *Exp. Cell Res.* 2006, *312*, 363–373.

[28] Zhou, D., Song, Z. H., *FEBS Lett.* 2002, *525*, 164–168.

[29] Zhao, Y., Yuan, Z., Liu, Y., Xue, J., Yuling, T., Weimin, L., Weiping, Z., Yan, S., Wei, X., Xiao, L., Tao, C., *J. Cardiovasc. Pharmacol.* 2010, *55*, 292–298.

[30] Lehmann, C., Kianian, M., Zhou, J., Kuster, I., Kuschnereit, R., Whynot, S., Hung, O., Shukla, R., Johnston, B., Cerny, V., Pavlovic, D., Spassov, A., Kelly, M. E., *Crit. Care* 2012, *16*, R47.

[31] Ekblom, P., Lonai, P., Talts, J. F., *Matrix Biol.* 2003, *22*, 35–47.

[32] Pan, H., Yang, K., Zhang, J., Xu, Y., Yuan, Y., Zhang, X., Xu, W., *J. Enzyme Inhib. Med. Chem.* 2012, 1–10.

[33] Pei, K. L., Yuan, Y., Qin, S. H., Wang, Y., Zhou, I., Zhang, H. L., Qu, X. J., Cui, S. X., *Cancer Chemother. Pharmacol.* 2012, *69*, 1029–1038.

[34] Ikeda, N., Nakajima, Y., Tokuhara, T., Hattori, N., Sho, M., Kanehiro, H., Miyake, M., *Clin. Cancer Res.* 2003, *9*, 1503–1508.

[35] Ku, N. O., Omary, M. B., *J. Cell Biol.* 1994, *127*, 161–171.

[36] Ku, N. O., Liao, J., Omary, M. B., *EMBO J.* 1998, *17*, 1892–1906.

[37] Schutte, B., Henfling, M., Kolgen, W., Bouman, M., Meex, S., Leers, M. PG., Nap, M., Björklund, V., Björklund, P., Björklund, B., Lane, E. B., Omary, M. B., Jörnvall, H., Ramaekers, F. C. S., *Exp. Cell Res.* 2004, *297*, 11–26.

[38] Dhanasekaran, S. M., Barrette, T. R., Ghosh, D., Shah, R., Varambally, S., Kurachi, K., Pienta, K. J., Mark A. Rubin, M. A., Chinnaiyan, A. M., *Nature* 2001, *412*, 822–826.

[39] Kang, S. Y., Halvorsen, O. J., Gravdal, K., Bhattacharya, N., Lee, J. M., Liu, N. W., Johnston, B. T., Johnston, A. B., Haukaas, S. A., Aamodt, K., Yoo, S., Akslen, L. A., Watnick, R. S., *Proc. Natl. Acad. Sci. USA* 2009, *106*, 12115–12120.

[40] Campana, W. M., Hiraiwa, M., Addison, K. C., O'Brien, J. S., *Biochem. Biophys. Res. Commun.* 1996, *229*, 706–712.

[41] Calvaruso, G., Pellerito, O., Notaro, A., Giuliano, M., *Int. J. Oncol.* 2012, *41*, 407–413.

[42] Longatti, A., Orsi, A., Tooze, S. A., *Cell Res.* 2010, *20*, 1181–1184.

[43] Millward, M., Price, T., Townsend, A., Sweeney, C., Spencer, A., Sukumaran, S., Longenecker, A., Lee, L., Lay, A., Sharma, G., Gemmill, R. M., Drabkin, H. A., Lloyd, G. K., Neuteboom, S. T. C., McConkey, D. J., Palladino, M.A., Spear, M. A., *Invest. New Drugs* 2012, *30*, 2303–2317.

[44] Hah, Y. S., Noh, H. S., Ha, J. H., Ahn, J. S., Hahm, J. R., Cho, H. Y., Kim, D. R., *Cancer Lett.* 2012, *323*, 208–214.

[45] Bosis, E., Nachliel, E., Cohen, T., Takeda, Y., Ito, Y., Bar-Nun, S., Gutman, M., *Biochemistry* 2008, *47*, 10970–10980.

[46] Wang, H. T., Lee, H. I., Guo, J. H., Chen, S. H., Liao, Z. H., Huang, K. W., Torng, P. L., Hwang, L. H., *Int. J. Cancer* 2012, *130*, 2892–2902.

[47] Lu, Y. C., Chen, C. N., Wang, B., Hsu, W. M., Chen, S. T., Chang, K. J., Chang, C., Lee, H., *Am. J. Pathol.* 2011, *179*, 1425–1433.

[48] Rodriguez-Navarro, J. A., Cuervo, A. M., *Autophagy* 2012, *8*, 1152–1154.

[49] Sahu, R., Kaushik, S., Clement, C. C., Cannizzo, E. S., Scharf, B., Follenzi, A., Potolicchio, I., Nieves, E., Cuervo, A. M., Santambrogio, L., *Dev. Cell* 2011, *20*, 131–139.

[50] Yabu, T., Imamura, S., Mohammed, M. S., Touhata, K., Minami, T., Terayama, M., Yamashita, M., *FEBS J.* 2011, *278*, 673–685.

[51] Joo, J. H., Dorsey, F. C., Joshi, A., Hennessy-Walters, K. M., Rose, K. L., McCastlain, K., Zhang, J., Iyengar, R., Jung, C. H., Suen, D. F., Steeves, M. A., Yang, C. Y., Prater, S. M., Kim, D. H., Thompson, C. B., Youle, R. J., Ney, P. A., Cleveland, J. L., Kundu, M., *Mol. Cell.* 2011, *43*, 572–585.

[52] Sanchez-Arago, M., Cuezva, J. M., *J. Transl. Med.* 2011, *9*, 19.

[53] Mikuriya, K., Kuramitsu, Y., Ryozawa, S., Fujimoto, M., Mori, S., Oka, M., Hamano, K., Okita, K., Sakaida, I., Nakamura, K., *Int. J. Oncol.* 2007, *30*, 849–855.

[54] Cook, A. J., Gurard-Levin, Z. A., Vassias, I., Almouzni, G., *Mol. Cell.* 2011, *44*, 918–927.

[55] Li, Y., Wan, O. W., Xie, W., Chung, K. K., *Neuroscience* 2011, *199*, 346–358.

[56] Reef, S., Shifman, O., Oren, M., Kimchi, A., *Oncogene* 2007, *26*, 6677–6683.

[57] Reef, S., Kimchi, A., *Autophagy* 2006, *2*, 328–330.

[58] Itahana, K., Zhang, Y., *Cancer Cell* 2008, *13*, 542–553.

